AMERICAN SOCIETY FOR MICROBIOLOGY | Journal of Virology®

PATHOGENESIS AND IMMUNITY

Systemic Expression of a Viral RdRP Protects against Retrovirus Infection and Disease

Caitlin M. Miller,[a] Bradley S. Barrett,[a] Jianfang Chen,[a] James H. Morrison,[a] Caleb Radomile,[a] Mario L. Santiago,[a] Eric M. Poeschla[a]

[a]Division of Infectious Diseases, Department of Medicine, School of Medicine, University of Colorado Anschutz Medical Center, Aurora, Colorado, USA

ABSTRACT The innate immune system is normally programmed for immediate but transient upregulation in response to invading pathogens, and interferon (IFN)-stimulated gene (ISG) activation is a central feature. In contrast, chronic innate immune system activation is typically associated with autoimmunity and a broad array of autoinflammatory diseases that include the interferonopathies. Here, we studied retroviral susceptibility in a transgenic mouse model with lifelong innate immune system hyperactivation. The mice transgenically express low levels of a picornaviral RNA-dependent RNA polymerase (RdRP), which synthesizes double-stranded RNAs that are sensed by melanoma differentiation-associated protein 5 (MDA5) to trigger constitutive upregulation of many ISGs. However, in striking counterpoint to the paradigm established by numerous human and murine examples of ISG hyperactivation, including constitutive MDA5 activation, they lack autoinflammatory sequelae. RdRP-transgenic mice (RdRP mice) resist infection and disease caused by several pathogenic RNA and DNA viruses. However, retroviruses are sensed through other mechanisms, persist in the host, and have distinctive replication and immunity-evading properties. We infected RdRP mice and wild-type (WT) mice with various doses of a pathogenic retrovirus (Friend virus) and assessed immune parameters and disease at 1, 4, and 8 weeks. Compared to WT mice, RdRP mice had significantly reduced splenomegaly, viral loads, and infection of multiple target cell types in the spleen and the bone marrow. During chronic infection, RdRP mice had 2.35 ± 0.66 $\log_{10}$ lower circulating viral RNA than WT. Protection required ongoing type I IFN signaling. The results show that the reconfigured RdRP mouse innate immune system substantially reduced retroviral replication, set point, and pathogenesis.

IMPORTANCE Immune control of retroviruses is notoriously difficult, a fundamental problem that has been most clinically consequential with the HIV-1 pandemic. As humans expand further into previously uninhabited areas, the likelihood of new zoonotic retroviral exposures increases. The role of the innate immune system, including ISGs, in controlling retroviral infections is currently an area of intensive study. This work provides evidence that a primed innate immune system is an effective defense against retroviral pathogenesis, resulting in reduced viral replication and burden of disease outcomes. RdRP mice also had considerably lower Friend retrovirus (FV) viremia. The results could have implications for harnessing ISG responses to reduce transmission or control pathogenesis of human retroviral pathogens.

KEYWORDS Friend virus, MDA5, retroviral pathogenesis, retroviruses, innate immunity, mouse model

The innate immune system must maintain a delicate balance between mounting an adequate host defense and causing excessive tissue damage (1, 2). Chronic, dysregulated activation characteristically results in a number of detrimental effects and is a cause of diverse autoimmune diseases (1). The innate antiviral response is a frontline defense that operates briefly at the earliest time point in the primary pathogen-infected

Citation Miller CM, Barrett BS, Chen J, Morrison JH, Radomile C, Santiago ML, Poeschla EM. 2020. Systemic expression of a viral RdRP protects against retrovirus infection and disease. J Virol 94:e00071-20. https://doi.org/10.1128/JVI.00071-20.

Editor Viviana Simon, Icahn School of Medicine at Mount Sinai

Address correspondence to Eric M. Poeschla, eric.poeschla@ucdenver.edu.

Received 14 January 2020
Accepted 7 February 2020
Accepted manuscript posted online 12 February 2020
Published 16 April 2020

cell or adjacent cells until adaptive antigen-specific immunity can generate antibodies and T cell responses. These transient, rapidly acting and often cell-autonomous defenses comprise a unique set of innate immune pathways driven by the detection of certain conserved viral components, typically nucleic acids (3). Double-stranded RNAs (dsRNAs) and single- and double-stranded DNAs that arrive in areas of the cell where they are normally excluded (e.g., RNA in an endosome) are signals of early viral infection (3). Mammalian cells have evolved sensors to detect these patterns early in order to trigger the production of type I interferons (IFNs) (3). The latter will then signal, in both autocrine and paracrine fashion, to upregulate hundreds of interferon-stimulated genes (ISGs), which act via diverse mechanisms to inhibit viral replication (2).

While transient expression of ISGs is crucial for combatting infection, a sustained ISG response can be damaging to the host (2). Chronic production of type I IFN and/or upregulation of ISGs is associated with multiple autoimmune diseases that include systemic lupus erythematosus (SLE), Aicardi-Goutières syndrome, Singleton-Merten syndrome, and retinal vasculopathy with cerebral leukodystrophy (1). Strong evidence links these diseases, which can be grouped broadly under the umbrella of "interferonopathies," to aberrant sensing of host nucleic acids as foreign (1, 4).

We previously described a unique murine model of chronic, systemic innate immune activation with ISG upregulation, which surprisingly does not result in autoimmune or inflammatory disease (5). RdRP-transgenic mice (RdRP mice) transgenically express low levels of the picornaviral RdRP from Theiler's murine encephalomyelitis virus (TMEV) (RdRP mRNA fragments per kilobase per million [FPKM] values are 1 to 2) (data not shown), the expression of which is driven by the tissue-nonspecific human ubiquitin C promoter (5–7). During the viral life cycle, the picornaviral RdRP is normally sequestered within membrane-wrapped replication factories (8, 9). When expressed unsequestered in the RdRP mouse, the RdRP templates on host cell RNAs to synthesize dsRNA, which then triggers chronic activation of cytosolic RNA-sensing pathways via melanoma differentiation-associated protein 5 (MDA5) and, downstream, mitochondrial antiviral-signaling protein (MAVS) (5). The exact RNAs synthesized are under investigation, but dsRNAs are strongly implicated by the intrinsic properties of the enzyme, our detection of elevated dsRNA levels in RdRP mouse tissue, and our previous genetic crosses with defined knockout strains that established the mechanism to be strictly MDA5 and MAVS dependent. The outcome of this MDA5/MAVs-mediated signaling pathway is lifelong, marked upregulation of dozens of antiviral ISGs, some by more than 100-fold (5). The type I interferon receptor is also required, but the mice do not have elevations in interferon mRNAs or proteins (5).

This stable ISG upregulation state is protective against the diseases caused by two picornaviruses (TMEV itself as well as encephalomyocarditis virus), a negative-strand RNA virus (vesicular stomatitis virus), and a herpesvirus (pseudorabies virus) (5–7). Importantly, additional crosses showed the elevated ISG signature and viral disease protection are adaptive immune system (RAG-1) independent, and also Toll-like receptor 3 (TLR3) and IFN-γ receptor independent (5).

Retroviruses have distinctive replication cycles and immune evasion properties compared to RNA viruses and DNA viruses. During retroviral replication, two copies of single-stranded (ssRNA) genome in the incoming particle are converted to dsDNA during reverse transcription in the target cell. This DNA becomes integrated into the host genome, resulting in permanent, lifelong infection (10). Innate sensing mechanisms for both RNA (TLR3, TLR7) and DNA (cyclic GMP-AMP synthase [cGAS], interferon gamma-inducible protein 16 [IFI16], and stimulator of interferon genes [STING]) have been described for retroviruses (11–16), with the cellular level of the three-prime repair exonuclease 1 (TREX1) being important for cGAS sensing (17). Retroviruses characteristically have a complex relationship with the host immune system, since immune cells themselves are frequently the targets of infection (18, 19). Accordingly, retroviral infection can cause progressive immunodeficiency or leukemic-like expansion of host immune cell subsets (18, 19). The most notable human retroviral pathogens are human immunodeficiency virus type 1 (HIV-1) and human T cell lymphotropic virus 1 (HTLV-1).

Both viruses are the cause of persistent human pandemics that have affected millions worldwide. Practically applicable cures or vaccines remain elusive for both.

Mice are useful and accessible animals for studying immunity to viruses. However, HIV-1 does not infect mice, and while HTLV-1 can infect rodents, viral pathology does not occur without extensive manipulations of the host immune system, which confound studies of immune response/control (20). In contrast, mice are readily infected with mouse-specific retroviruses such as murine leukemia viruses (MLVs). In particular, infection studies of various strains of mice with Friend retrovirus (FV) have, since the 1950s, provided breakthrough understanding of mechanisms of host genetic control (21). FV is a complex of two retroviruses: a replication-competent Friend MLV, which acts as a helper virus with a functional envelope protein, and a replication-defective spleen focus-forming virus (SFFV), which encodes a modified form of envelope, gp55P, which can activate the erythropoietin receptor in conjunction with an Fv2-susceptible allele (22). Infection of mice with an Fv2-susceptible allele results in severe splenomegaly due to uncontrolled proliferation of erythroblast precursors. Subsequently, erythroleukemia develops due to insertional mutagenesis. Critical genes that control FV infection such as the postentry restriction factor *Fv1*, the major histocompatibility locus, and the retroviral deaminase apolipoprotein B mRNA editing enzyme, catalytic polypeptide-like (APOBEC)/*Rfv3* were found to be highly relevant to HIV-1 infection; for a review, see reference 23. Here, we used the FV model to determine the impact of low-level transgenic RdRP expression on retroviral pathogenesis *in vivo*. Our results suggest that a broad ISG response that is constitutive but not autoinflammatory disorder provoking may have potential for protection against pathogenic human retrovirus infection.

RESULTS

RdRP protects against high-dose FV infection. RdRP-transgenic mice were created in the FVB mouse strain, which harbors the Fv2-susceptibility allele (24). Thus, we expected FVB mice to be highly prone to FV-induced splenomegaly. Given the strong resistance of RdRP mice to infection by several DNA and RNA viruses (5–7), we initially used a high-dose inoculum (10,000 spleen focus-forming units [SFFU]) to test if RdRP mice completely resist FV infection. We used FV stocks lacking lactate dehydrogenase-elevating virus (LDV), which triggers a strong type I IFN response (25, 26). To determine the level of infection, spleen, serum, and bone marrow were harvested at 7 days postinfection (dpi). Circulating plasma viral loads were quantified using quantitative RNA PCR (qPCR), and spleens were weighed to assess splenomegaly, which is consequent to the erythroleukemia that FV causes and is a frequent proximate cause of mortality when splenic rupture occurs.

We observed substantially lower spleen sizes and circulating plasma viral loads in RdRP mice than in wild-type (WT) mice at 7 dpi (Fig. 1A and B). Thus, RdRP mice are not entirely immune to high-dose FV infection, but they control the virus better than their WT counterparts. We next examined the level of infection in immune cell subsets by flow cytometry. In addition to erythroblasts, FV is able to infect B cells, T cells, and dendritic cells (DCs) in both bone marrow and spleen (27, 28). The bone marrow is the initial site of infection after FV inoculation and the site of leukemogenesis of erythrocyte precursor cells (27–29). We observed relatively small differences in the level of infection of cellular subsets in the bone marrow (Fig. 1C). However, we did identify a significant decrease in infection of T cells and B cells in RdRP mice compared to WT mice (Fig. 1C). The effects on splenic subsets were more significant. We observed decreased infection of total splenocytes, erythroblasts, T cells, and B cells in RdRP mice compared to WT controls (Fig. 1D). Taken together, these results show that RdRP mice significantly controlled acute-phase FV infection compared to WT counterparts after a high-dose challenge.

Canonical ISG and cytokine mRNA assessments in spleen and bone marrow. Infection with LDV-free FV stimulates a very weak ISG response. Thus, RdRP expression may have protected mice against high-dose FV infection by compensating for this low

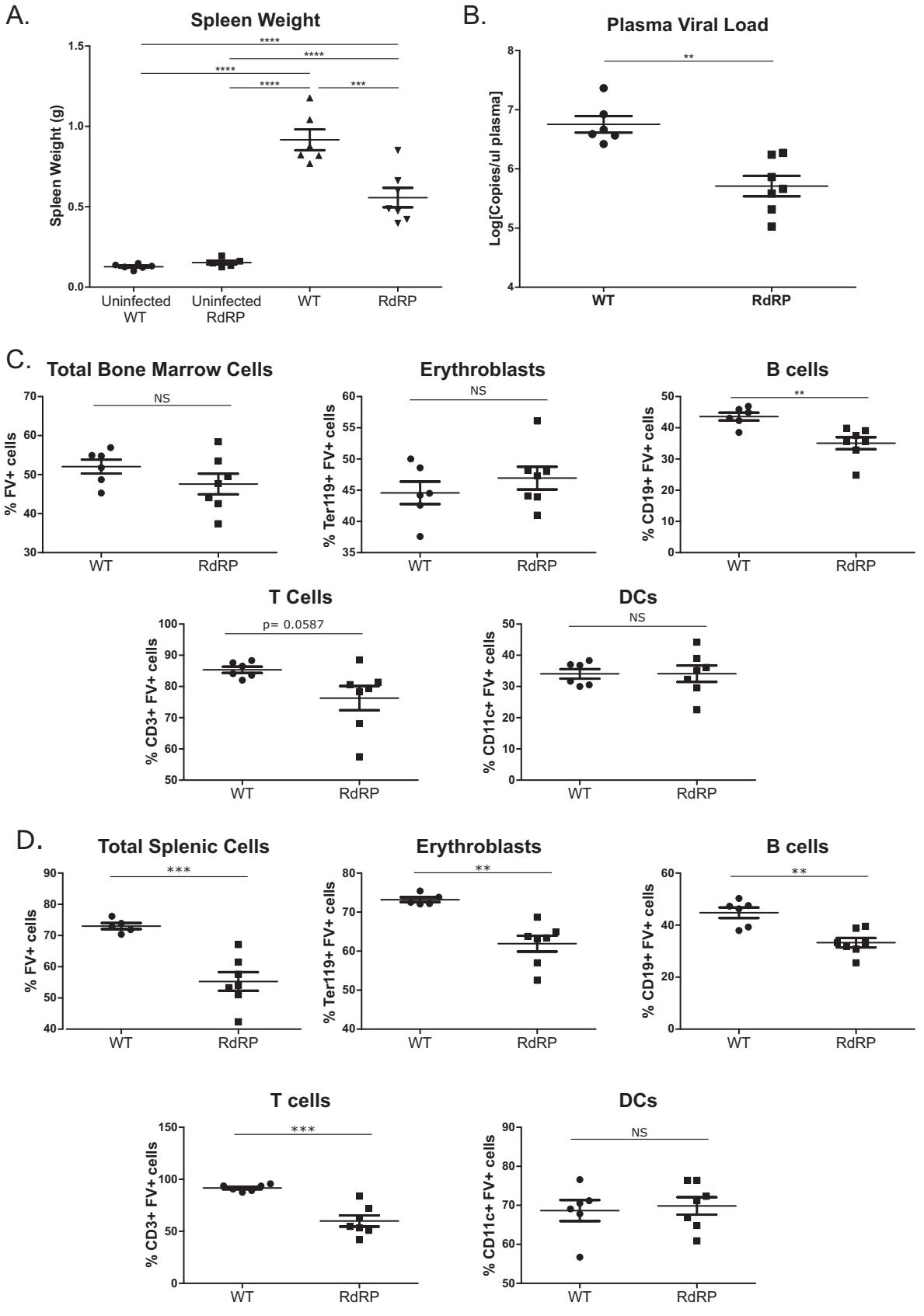

FIG 1 Differences in high-dose acute phase FV infection in WT and RdRP mice. Mixed-gender, 13- to 16-week-old mice were infected with 10,000 PFU B-tropic FV by retroorbital injection. (A) At 7 dpi, spleens were harvested for weight analysis to determine the level of

(Continued on next page)

ISG response. We began to investigate this question by performing qPCR for selected canonical ISGs on splenic tissue from FV-infected and FV-uninfected WT and RdRP mice. As shown in Fig. 2A, and congruent with the prior data (5), in uninfected RdRP mice, there was elevated expression of the representative ISGs Ifit1 (interferon-induced protein with tetratricopeptide repeats 1) and Oasl2 (2′-5′-oligoadenylate synthase-like protein 2). These genes were chosen as representative of the generally upregulated ISG response observed in RdRP mice, since we have previously shown them to be highly upregulated and easily measurable (5). After FV infection, Ifit1 and Oasl2 expression remained significantly elevated in infected RdRP mice relative to infected WT mice. Interestingly, FV infection of RdRP mice reduced Ifit1 and Oasl2 expression, suggesting that FV infection is able to partially inhibit type I IFN responses, similar to immunosuppressive effects reported by others (30) (Fig. 2A). We also measured expression of the RdRP transgene itself. Interestingly, FV infection reduced expression of the RdRP mRNA in splenic tissue (Fig. 2B), which may explain the mild drop in ISG expression in RdRP mice after infection.

We also screened for proinflammatory cytokine changes during FV infection. We reported previously that RdRP expression does not result in a tissue inflammatory response, both when expressed alone or in response to encephalomyocarditis virus (EMCV) infection. Instead, the responses are confined to upregulation of ISGs (5). To test whether FV infection combined with RdRP expression would differ in this regard, we measured the relative expression of mRNAs for two classical proinflammatory cytokines, tumor necrosis factor alpha (TNF-α) and interleukin 6 (IL-6). In both infected and uninfected mice, we observed no RdRP genotype-specific differences in TNF-α and IL-6 transcripts. Both proinflammatory gene mRNAs were depressed in FV-infected mice compared to uninfected mice (Fig. 2C). These results suggest that RdRP mice do not control infection through the induction of a proinflammatory response. In bone marrow, analogous investigations revealed a largely similar pattern, although in this tissue, there was not a suppression of Ifit1, Oasl2, or Isg15 transcripts by FV like that observed in splenic tissue, and proinflammatory transcripts were largely unchanged by either the RdRP transgenic state or the virus (Fig. 2D and E).

RdRP expression is protective during chronic Friend virus infection. We then turned to the issue of whether the RdRP-mediated antiviral effects observed extend to the chronic stage of FV infection. In view of the high levels of splenomegaly that occurred at 7 dpi after high-dose (10,000 SFFU) FV infections, we reduced the inoculum to 2,500 SFFU and evaluated infection sequelae at 28 dpi. Several mice ($n = 4$ out of 20) had to be prematurely removed from the study due to morbidity or mortality (at 10 and 23 dpi for WT and 12 and 22 dpi for RdRP), indicating that this dose can still cause severe disease. At 28 dpi, we harvested spleens for weight assessment and blood for plasma viral load quantification. Among mice that survived, there was a significant decrease in spleen size in RdRP mice compared with WT mice (Fig. 3A and C). The distribution of spleen sizes was bimodal, suggesting that some RdRP mice may be recovering from infection (spleens under 1.0 g) and some may have progressed to disseminated disease (spleens over 1.0 g), with the majority of mice falling into the less ill group. When we measured circulating plasma viral load, we observed similar results; RdRP mice had significantly decreased plasma viral loads (2.35 ± 0.66 $\log_{10}$ lower) (Fig. 3B). Again, we noted a wide distribution in RdRP mice, ranging from 10^5 to 10^6 (similar to all WT mice measured), down to below the limit of detection (less than 100 copies/μl). When we plotted spleen weight against plasma viral load, we observed a

FIG 1 Legend (Continued)
splenomegaly. (B) Plasma was simultaneously obtained to determine plasma viral load via qPCR. (C) Bone marrow was harvested, and a single-cell suspension was created to determine the overall amount of FV infection, as well as the level of FV infection in erythroblasts, B cells, T cells, and DCs via flow cytometry. (D) As in panel C, single-cell solutions were prepared from spleen, and the overall infection level, as well as infection of erythroblasts, B cells, T cells, and DCs, was determined using flow cytometry. For all experiments shown, $n = 6$ for WT uninfected and WT, $n = 5$ for RdRP uninfected, and $n = 7$ for RdRP. A one-way ANOVA with a Tukey test was used to analyze data in panel A, and student's *t* tests were used to analyze data in panels B through D. *, $P < 0.05$; **, $P < 0.01$; ***, $P < 0.001$; ****, $P < 0.0001$. Data in panel B were log transformed prior to statistical analysis.

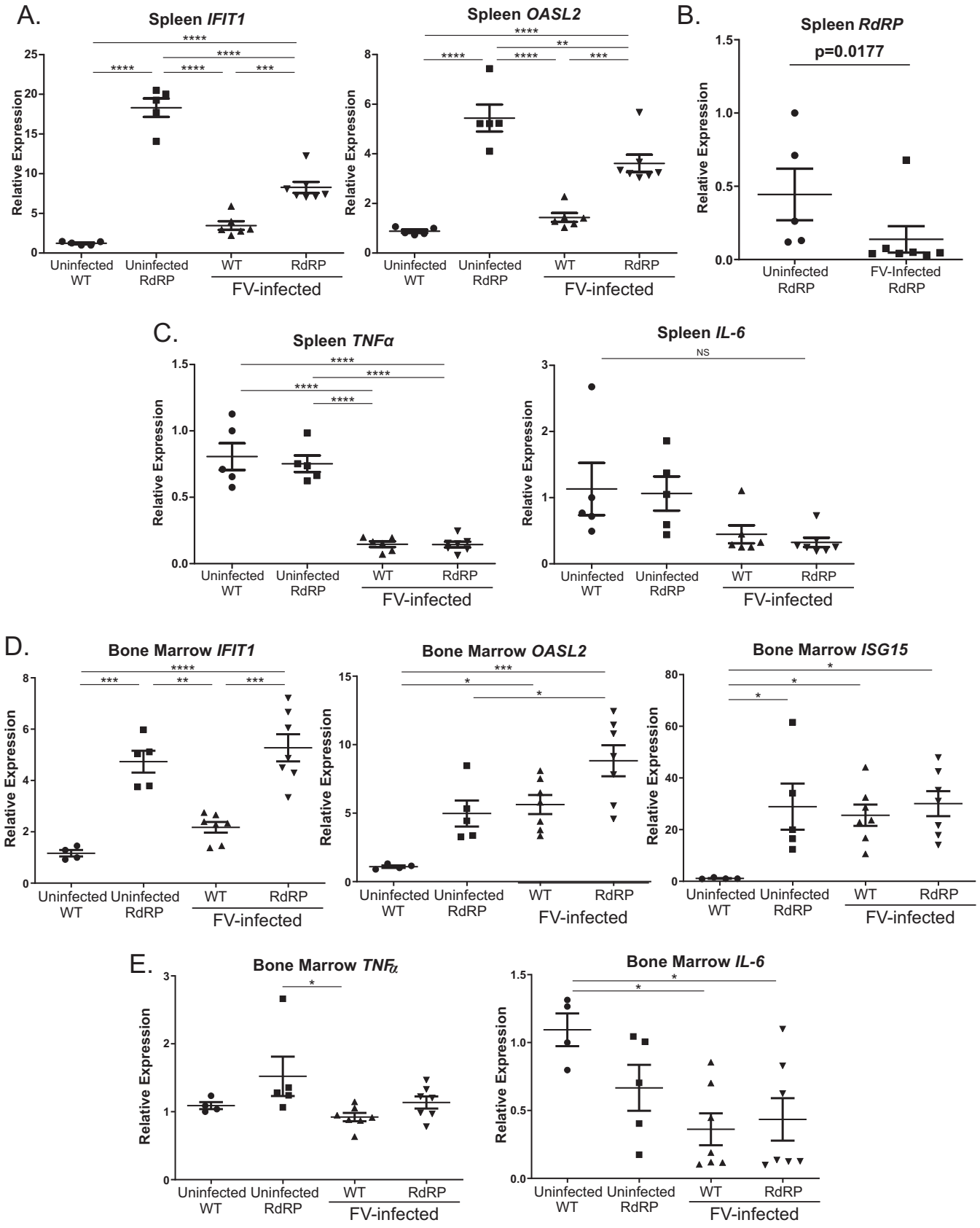

FIG 2 Correlates of protection in RdRP mice during acute-phase infection. Total RNA isolated from spleen (A, B, and C) and bone marrow (D, E) from infected and uninfected mice described in Fig. 1 was used for reverse transcription-quantitative PCR (qRT-PCR) analysis of differences in mRNA expression. (A) ISGs Ifit1 and Oasl2

(Continued on next page)

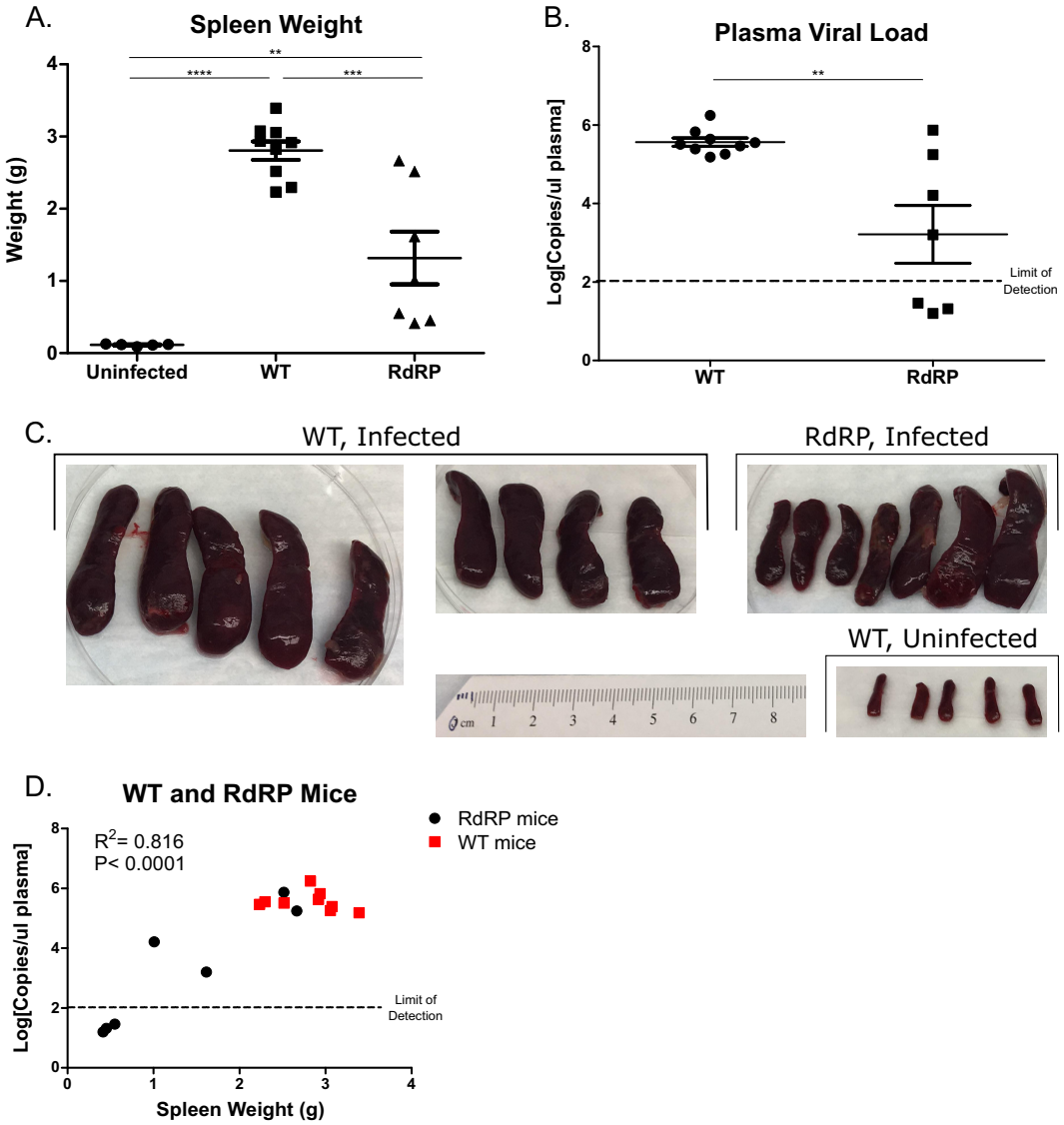

FIG 3 RdRP mice show resistance and signs of recovery during low-dose chronic FV infection. Mixed-gender mice 16 to 17 weeks of age were retro-orbitally injected with 2,500 PFU of B-tropic FV. At 4 weeks after infection, spleens were harvested to assess splenomegaly by weight (A) and photography (C), and plasma was harvested to determine plasma viral load by qPCR (B). (D) Correlation analysis of plasma viral load versus spleen weight. Plasma viral load was log transformed before analysis, and correlation analysis was done to determine significance. For all experiments, $n = 5$ for uninfected, $n = 9$ for WT, and $n = 7$ for RdRP. For spleen weights, data were analyzed using a one-way ANOVA followed by a Tukey test to determine significance. For plasma viral loads, data were log transformed and then analyzed using a Student's t test. For correlation analysis (D), plasma viral load was log transformed, and correlation analysis and a Pearson's test was run. *, $P < 0.05$; **, $P < 0.01$; ***, $P < 0.001$; ****, $P < 0.0001$.

strong correlation for all mice (Fig. 3D). RdRP mice with spleen weights under 2.0 g had low to undetectable circulating virus, while animals with spleen weights over 2.0 g had high levels of circulating virus; all WT spleens weighed over 2.0 g (Fig. 3D). Together, these data reveal that RdRP expression reduced splenomegaly and viremia at a chronic infection time point after low-dose FV challenge.

FIG 2 Legend (Continued)
in spleen. We observed a similar baseline 5- to 10-fold upregulation of Isg15 (interferon-stimulated gene 15) mRNA in uninfected RdRP mice spleens (data not shown). (B) RdRP mRNA expression. (C) The proinflammatory cytokines TNF-α and IL-6 were similarly assessed. For experiments shown, $n = 6$ for WT uninfected and WT, $n = 5$ for RdRP uninfected, and $n = 7$ for RdRP. (D, E) Similar assays for ISG expression (D) or proinflammatory cytokine expression (E) were performed on bone marrow infected with 1,000-PFU B-tropic FV, harvested on 7 dpi; $n = 4$ for uninfected WT, $n = 5$ for uninfected RdRP, and $n = 7$ for infected WT and RdRP. Data were analyzed using a one-way ANOVA followed by a Tukey test for individual comparison (*, $P < 0.05$; **, $P < 0.01$; ***, $P < 0.001$; ****, $P < 0.0001$).

Increased ISG levels in the spleens of infected RdRP mice are associated with retroviral control. As previously shown in Fig. 2, in both spleen and bone marrow, RdRP expression results in drastically upregulated ISG expression without induction of proinflammatory cytokines prior to infection. We wanted to investigate whether there were other immunological differences in RdRP mice prior to infection, specifically in the various cellular subsets targeted by FV, which may be contributing to protection. FVB mice express the attenuated form of the APOBEC protein that is known to be a major determinant of FV susceptibility (31–33). The ISG tetherin/BST-2 also limits FV infection and has well-described antiviral roles in HIV pathogenesis (34–37). We measured cell surface BST-2 expression in various cellular subsets in the spleens of WT and RdRP mice as well as the overall percentages of different cellular subsets (Fig. 4A to C). When we examined baseline differences in cellular subsets, we observed minor changes in the quantities of B cells and T cells in RdRP mice compared to WT, with a decrease in the number of T cells and an increase in the number of B cells (Fig. 4A). We also observed increased expression of BST-2 in all cellular subsets examined (Fig. 4B and C), suggesting that all cells are responding to RdRP-mediated ISG upregulation. RdRP-mediated upregulation of BST-2 might be contributing to resistance to FV infection.

Finally, since we observed that during acute infection, DC subsets consistently showed no differences in infection in both the spleen and bone marrow (Fig. 1C and D), we wished to determine if there was an intrinsic difference in DC functionality in RdRP mice that might be causing this lack of DC resistance. Because we observed no differences in the overall quantities of DCs in RdRP mice (Fig. 4A), we quantified different subtypes of DCs. We observed a slight decrease in conventional DC1s (cDC), cDC2s, and plasmacytoid DCs (pDCs), and a trend toward an increase in monocytes (Fig. 4D). We also examined activation statuses of the DC subsets via CD80/CD86 staining. Only monocytes showed a significant difference in the amount of CD80/CD86 staining, with decreased expression on cells from RdRP mice at baseline (Fig. 4E). Monocytes are functionally less mature than DCs of various subsets, and they tend to act in a more inflammatory manner as a secondary response to infection or trauma (38, 39). A decrease in monocyte activation might be indicative of a lack of ability of the cells to differentiate into predecessor cells that include monocyte-derived DCs (moDCs) and macrophages (note moDCs were measured in Fig. 4F, and no significant change was observed, although data trended toward a decrease in RdRP mice; $P = 0.127$) and respond to stimuli, indicating infection or inflammation (39). Together, these data suggest a lack of functionality that might impact the ability of DCs to control FV infection.

Matched acute and chronic disease assessments to determine if RdRP mice recover from FV infection. The results described above support an inference that RdRP expression drives aspects of recovery from FV infection. To test this hypothesis, we designed an infection protocol that would allow evaluation of disease signs at both acute and chronic time points (Fig. 5A). Mice were inoculated with a lower dose of virus (1,000 SFFU), and a subset was euthanized at 7 dpi to determine acute disease sequelae. In these mice, we again observed a significant decrease in spleen size in RdRP mice compared to WT (Fig. 5B), similar to the previous high-dose acute infection experiments. Decreased splenomegaly corresponded with decreased infection overall in splenocytes (Fig. 5C). Interestingly, at this lower dose, we also observed a significant decrease in overall infection in the bone marrow (Fig. 5D), which is distinct from what we observed in the bone marrow after infection with high-dose (10,000 SFFU) FV challenge (Fig. 1). These results suggest that the protective effects against infection of this compartment mediated by the RdRP may be saturable at the high FV dose. Examining infection in different immune subsets in the spleen and bone marrow, we found that infection was reduced specifically in erythroblasts and T cells in the spleen (Fig. 5E). In the bone marrow, there was decreased FV infection of all subsets of cells examined in RdRP mice compared to WT (Fig. 5F), again in contrast to what we observed after high-dose infection (Fig. 1). These results indicate that, in addition to the

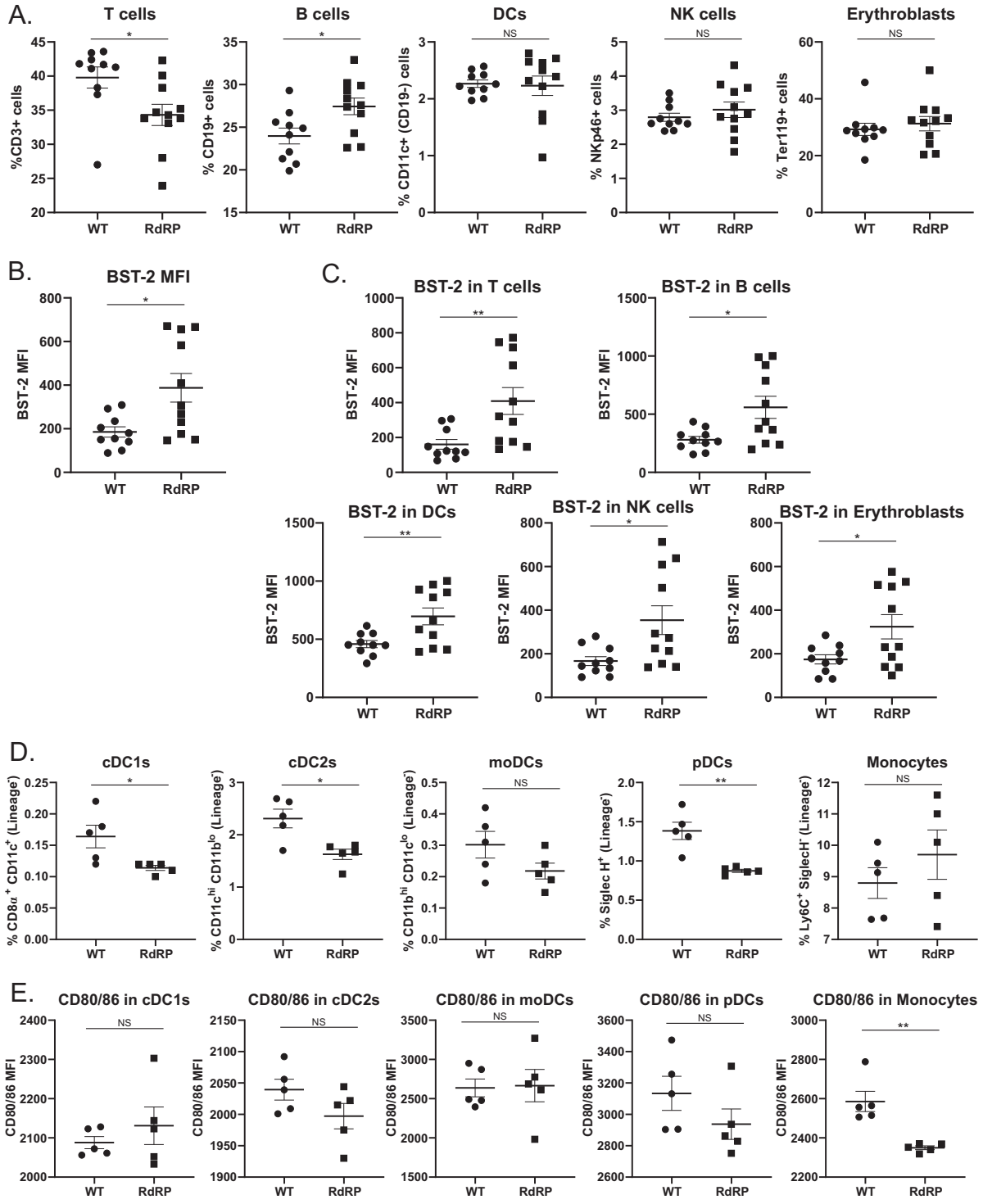

FIG 4 Correlates of protection in RdRP mice. (A) Total splenocytes from uninfected WT and RdRP mice stained for markers to identify T cells, B cells, DCs, natural killer (NK) cells, or erythroblasts. (B, C) MFI of BST-2 expression on total splenocytes (B) or on cellular subsets (C), stained as described in panel A. For WT, $n = 10$, and RdRP, $n = 11$. (D, E) RBC-lysed splenocytes were stained for DC subsets (D) and CD80/CD86 expression (E) to determine cellular activation status. In panels D and E, $n = 5$ for WT and 5 for RdRP. Data for all experiments were analyzed using an unpaired Student's t test. *, $P < 0.05$; **, $P < 0.01$; ***, $P < 0.001$; ****, $P < 0.0001$.

spleen, the RdRP mouse bone marrow is also relatively protected at a nonsaturating inoculum dose.

Matched chronic disease assessment reveals that RdRP drives recovery from viremia but not splenomegaly. We next determined disease outcomes in the remain-

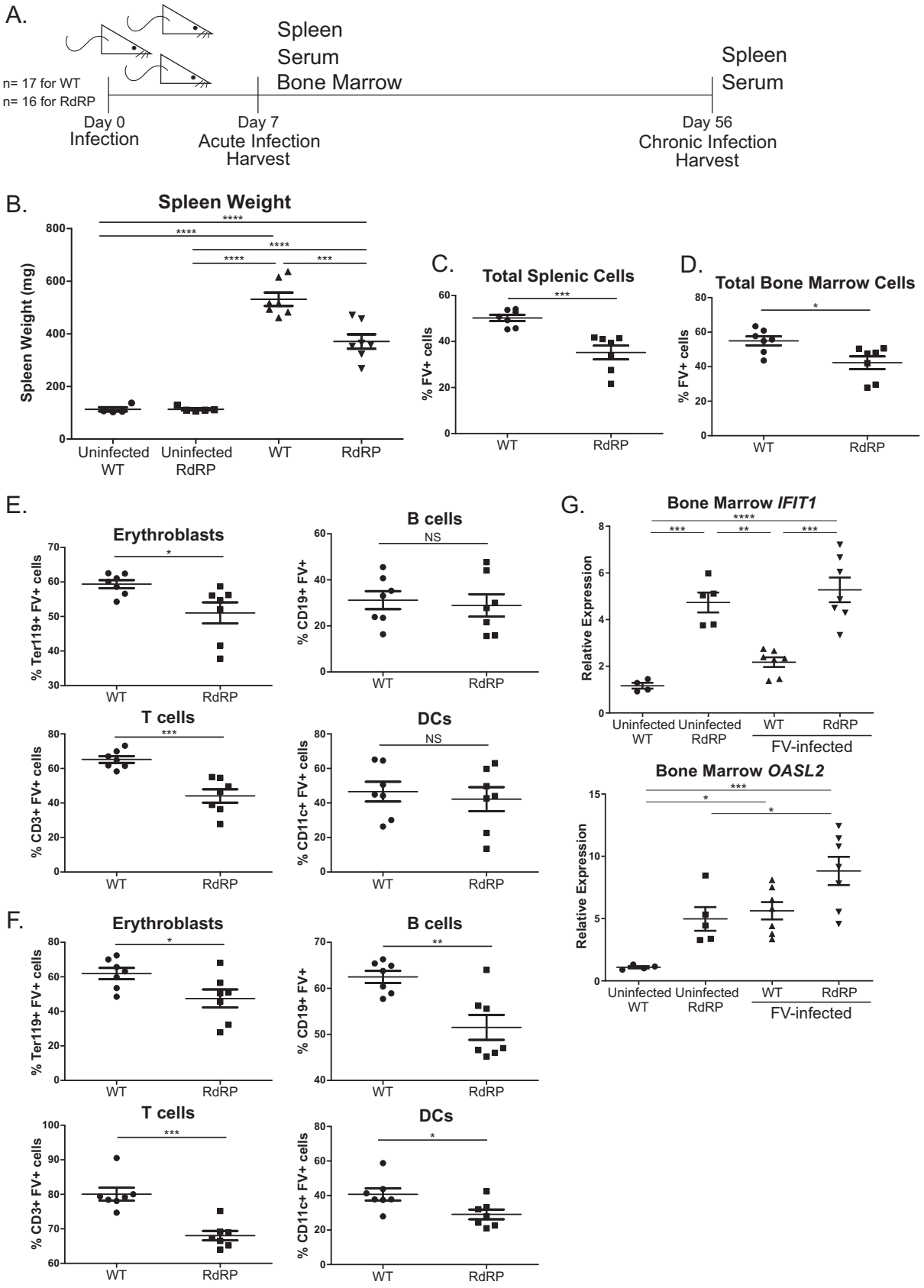

FIG 5 RdRP mice are resistant to low-dose FV during acute-phase time points. (A) Design of mouse infection experiments to determine recovery in RdRP mice. Mixed-gender mice 16 to 18 weeks of age were infected with 1,000 PFU virus and harvested for disease progression analysis at 1 and 8

(Continued on next page)

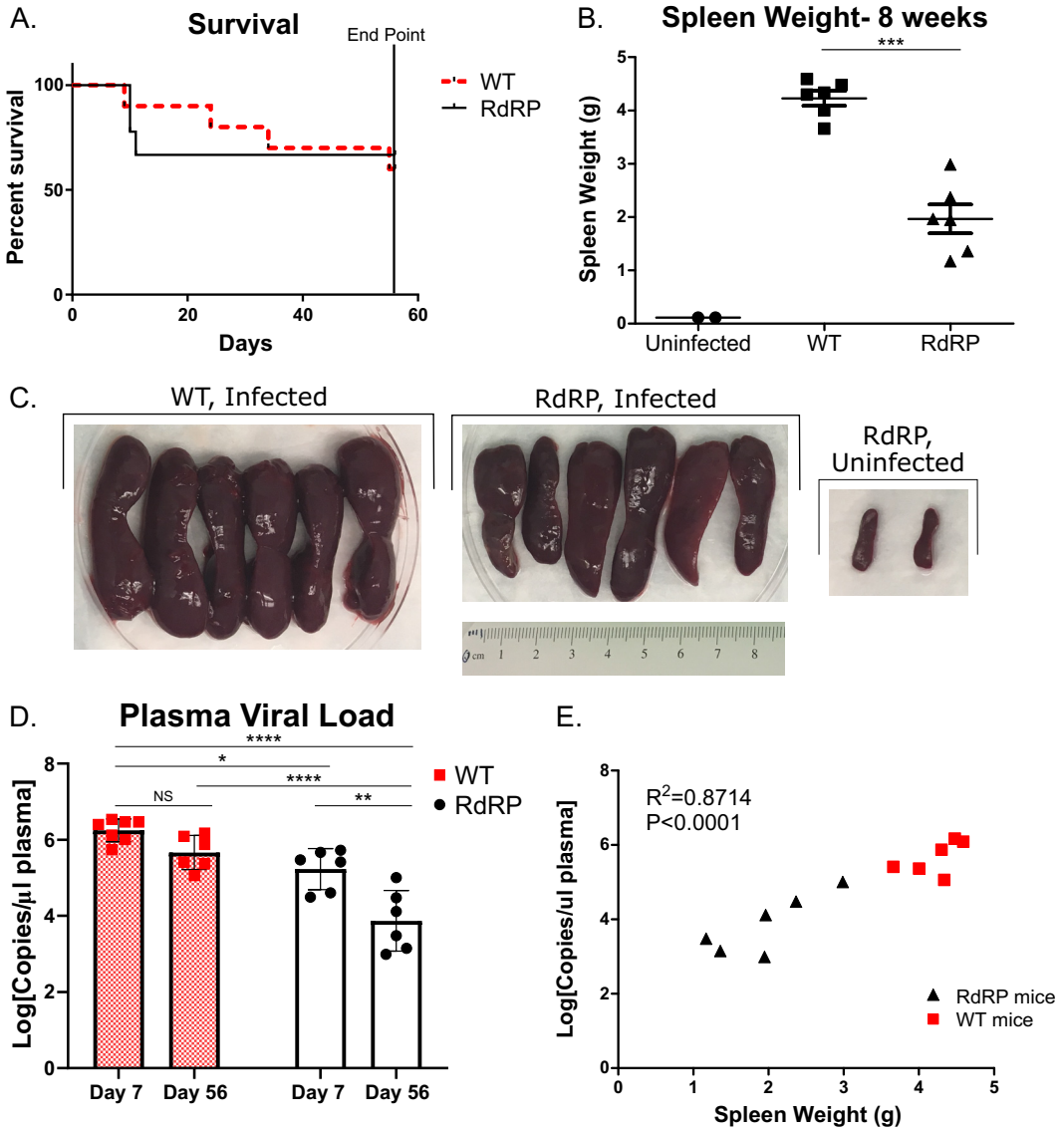

FIG 6 RdRP mice have reduced disease burden and exhibit recovery from viremia during chronic FV infection. (A) Survival differences in WT and RdRP mice infected as described in Fig. 5A over the course of 8 weeks (mice euthanized at 1 week were excluded from analysis). (B, C) Spleen weights and visual images of spleens of mice euthanized at 8 weeks postinfection. (D) Circulating plasma viral loads at both day 7 (acute) and day 56 (chronic) as quantified by qPCR. (E) Correlation of spleen weight and plasma viral load. Spleen weights were analyzed using a Student's *t* test to determine significance. Two uninfected mice were included in panels B and C to show baseline spleen size for comparison but were excluded from statistical analysis. Plasma viral load data were log transformed and then analyzed using a two-way ANOVA followed by a Sidak test to determine adjusted *P* values. Correlation analysis was done to determine significance in panel E. For all data shown, $n = 6$ for WT and RdRP mice, except day 7 data in D, where $n = 7$ for WT. *, $P < 0.05$; **, $P < 0.01$; ***, $P < 0.001$; ****, $P < 0.0001$.

ing mice at 56 dpi (i.e., at the final endpoint illustrated in Fig. 5A). As in the previous chronic disease experiment (Fig. 3), several mice had to be removed from the study due to morbidity or mortality (Fig. 6A). When we measured survival over the course of the 8 weeks, we did not find a significant difference in overall survival between WT and

FIG 5 Legend (Continued)

weeks after infection to assess matched acute and chronic disease. (B) Spleen weight harvested at 1 week postinfection. (C, E) Single-cell suspensions of splenocytes stained for overall FV infection level (C) and specific infection levels in erythroblasts, B cells, T cells, and DCs, determined by flow cytometry (E). (D, F) Single-cell suspensions of bone marrow cells were stained for overall infection (D) and specific infection in erythroblasts, B cells, T cells, and DCs (F), and analyzed by flow cytometry as in panels C and E. In all experiments, $n = 4$ for uninfected WT, $n = 5$ for uninfected RdRP, and $n = 7$ for both WT and RdRP. A one-way ANOVA followed by a Tukey test to determine significance was used to analyze spleen weight in panel B, and for all other analyses, a Student's *t* test was used to determine significance. *, $P < 0.05$; **, $P < 0.01$; ***, $P < 0.001$; ****, $P < 0.0001$.

RdRP mice (Fig. 6A). However, we observed a significant decrease in spleen weight and visually assessed splenomegaly in RdRP mice compared to WT (Fig. 6B and C). Average spleen weight was reduced by more than half (Fig. 6B). Despite the significant reductions in spleen size at 8 weeks, all infected mice exhibited marked splenomegaly and signs of disseminated erythroblastoma, suggesting that RdRP status alone does not permit full recovery from splenomegaly (Fig. 6).

To assess another recovery metric, we measured plasma viral loads at days 7 and 56 postinfection. This measurement has a correlate in HIV-1 viral load, which strongly determines HIV disease progression (40). The purpose was to determine if there were differences in viral load between WT and RdRP mice, not only within a harvest point but also over time. A decrease in plasma viral load from day 7 to day 56 within an infection group would suggest that those mice were beginning to recover from viremia, which can occur independently of control of erythroblastoma and recovery from splenomegaly. At each harvest point, we observed a significant decrease in circulating plasma viral load in RdRP compared to WT (Fig. 6D). Interestingly, we also observed a significant decrease in viral load in RdRP mice at day 56 compared to day 7 (Fig. 6D), which amounted to a mean 1.36-1$\log_{10}$ drop in circulating virus by day 56, signifying that RdRP mice are recovering from viremia. In contrast, in WT mice, significant decreases in circulating virus were not observed between harvest time points (Fig. 6D), indicating that this recovery is unique to RdRP mice. Additionally, when spleen weight was compared to plasma viral load at 56 dpi, we observed a significant correlation between weight and circulating virus (Fig. 6E), again confirming, as in Fig. 3D, that RdRP mice are better able to control FV infection at chronic disease time points. These results indicate that RdRP expression is able to reduce disease sequelae throughout the course of FV infection and drive recovery from viremia.

Neutralizing type I IFN signaling blocks RdRP-mediated resistance to FV infection. Lastly, we wanted to determine whether ongoing type I IFN signaling contributes to protection against FV. Previous studies have shown that knockout of the type I IFN receptor (IFNAR), which mediates all type I IFN signaling in mice (41), results in increased susceptibility to FV infection (25). In the RdRP mouse model, our previous crosses with similar IFNAR1$^{-/-}$ mice showed that type I IFN signaling is necessary for development of the augmented ISG expression profile of the RdRP mouse and for protection against EMCV (5). This is the case even though type I IFN mRNA and protein levels are not elevated in these mice (5). Here, the postdevelopmental situation was assessed by treating adult mice, prior to and during FV infection, with MAR1-5A, an anti-IFNAR1 monoclonal antibody that blocks receptor signaling (42), or an IgG control antibody (Fig. 7A). Such treatment reverses the broad ISG elevations of adult RdRP mice (data not shown). Mice were given an initial high dose (2.5 mg) of antibody via intraperitoneal injection in order to saturate whole-body expression of IFNAR and two follow-up doses to maintain ablation (Fig. 7A). This inhibited expression in both groups of a canonical ISG, Oasl2 (Fig. 7B).

After the antibody treatments, the mice were infected with 100 PFU of FV. This very low dose was chosen because of the likelihood of increased morbidity/mortality in the absence of functional type I IFN signaling (25). The mice were then euthanized at 7 dpi for disease evaluation. In MAR1-5A-treated mice, we observe increased spleen sizes and circulating plasma viral loads in RdRP mice compared to RdRP mice treated with control antibody (Fig. 7C and D). Note that the IFNAR1 blockade-caused increase in circulating viral load was an approximately 1.5-$\log_{10}$ difference in RdRP mice versus an approximately 0.5-$\log_{10}$ difference in WT mice, and the level was equivalent to that in the WT group, suggesting full reversal of the protective state (Fig. 7D). Total infection in both the spleen and bone marrow was increased in both WT and RdRP mice treated with MAR1-5A compared to RdRP mice treated with the control antibody (Fig. 7E and F). Individual cellular infection of T cell, DC, and erythroblast subsets in both the spleen and bone marrow also increased in MAR1-5A-treated RdRP mice compared with IgG-treated RdRP mice (Fig. 7G and H). Together, these results indicate that ongoing

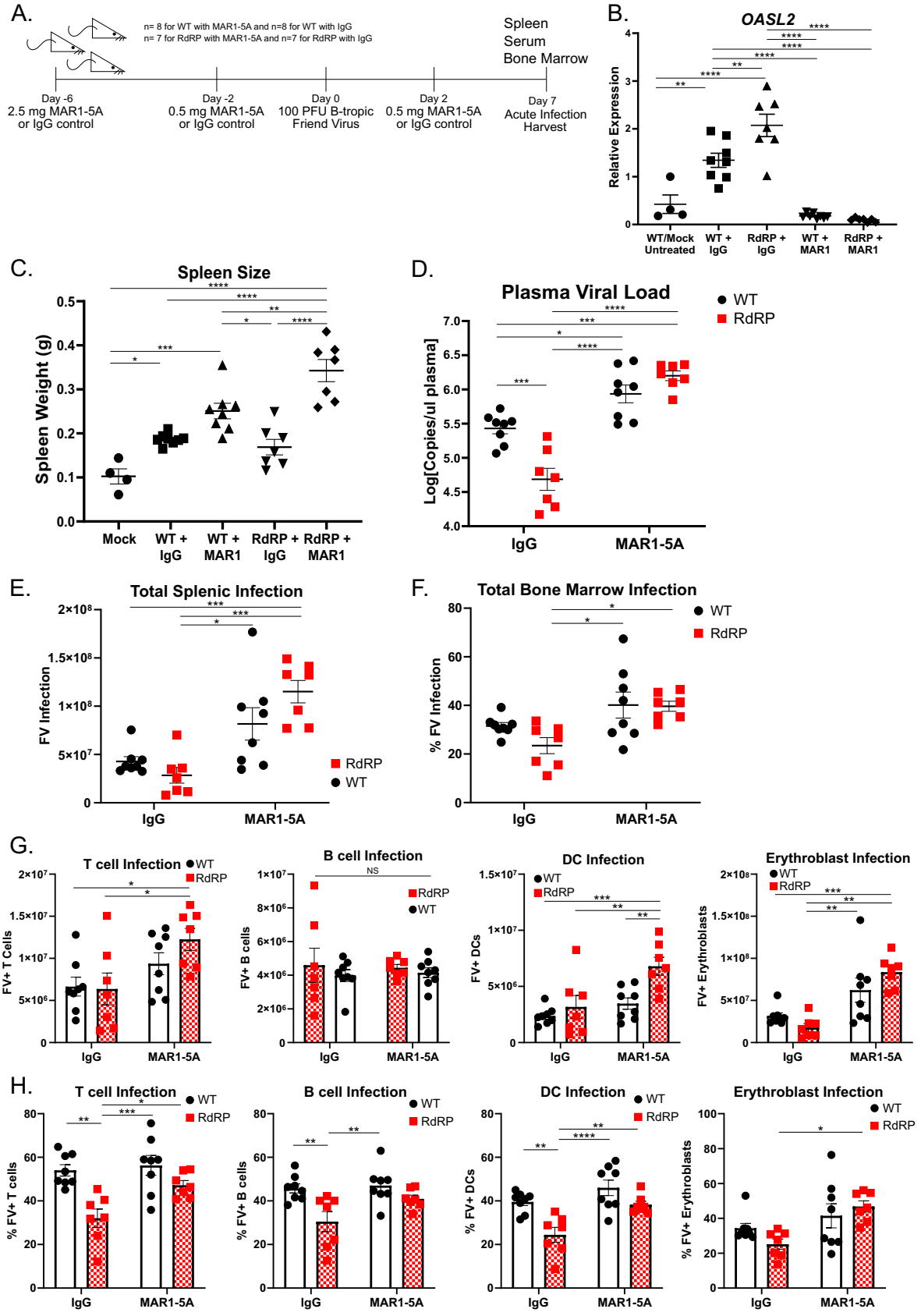

FIG 7 Blockage of IFN receptor signaling eliminates protection against FV infection in RdRP mice. (A) Experimental design of anti-IFNAR-treated mice for infection with 100 PFU FV. Mixed-gender mice were treated with MAR1-5A or IgG control at indicated doses and time points

(Continued on next page)

(postdevelopment) type I IFN signaling is required to limit FV replication and pathogenesis in RdRP mice.

DISCUSSION

Retroviruses have a distinctive life cycle and immune system evasion features and characteristically produce chronic infections that are abetted by the signature property of permanent integration into the host cell genome. Immune control of these viruses is notoriously difficult, a problem that has been most clinically consequential with the HIV-1 pandemic. Therapeutically, neither vaccine nor immune system-mediated control strategies have yet succeeded. The role of the innate immune system, including ISGs, in controlling retroviral infections is currently an area of intensive study. In this work, we demonstrate that low-level transgenic expression of a picornavirus RdRP, which results in substantial elevation of a broad panel of antiviral ISGs (5), was protective against acute and chronic retroviral infection in mice. This mouse synthesizes elevated levels of cellular dsRNA, which triggers chronic MDA5-MAVs activation, lifelong ISG upregulation, and consequent resistance to plus- and negative-strand RNA viruses and a DNA virus (5, 7). These effects are mouse strain independent and, of great interest, result in no discernible negative health effects or longevity costs (5). Normally, mice with activating mutations in MDA5 develop early, severe disease that is reflective of human autoimmune interferonopathies (1, 43, 44).

To date, we have tested resistance to rapidly replicating RNA and DNA viruses that cause transient infections and rapidly culminate in either virus clearance/latency or mouse death (5, 7). The RdRP mice very effectively control (and are fully resistant to the diseases caused by) the picornaviruses EMCV and TMEV (plus-strand RNA), the rhabdovirus vesicular stomatitis virus (VSV) (negative-strand RNA), and the swine alphaherpesvirus pseudorabies virus (PRV) (a DNA virus) (5, 7), but they have yet to be challenged with a retrovirus or any other virus that establishes prolonged, chronic replication in normal mice. Here, mice were infected with various doses of a highly pathogenic retrovirus (FV) and disease variables were assessed at both acute (1 week) and chronic (4 and 8 weeks) stages of infection. At all of the time points, we observed reduced circulating free virus in plasma and reduced splenomegaly resulting from disseminated erythroblastoma. Notably, at the FV doses we used, FV was not completely blocked, which is unique among the viruses tested in RdRP mice to date (5, 7). We did observe consistently lower circulating virus and disease signs over the course of infection, indicating that the RdRP reduces disease progression during chronic FV infection, contributing to lower morbidity and mortality. For example, at the 8-week time point, we found that the RdRP genotype was associated with significant recovery from FV viremia (Fig. 6D). Splenomegaly progressed in infected RdRP mice (compare weight values in Fig. 6B with values in Fig. 5B) but was still lower than in WT mice (Fig. 6B and C). The two processes are not necessarily linked during pathogenesis. Recovery from viremia but progression of splenomegaly indicates that RdRP mice dampen viral replication but do not block progression of the erythroblastoma once established. Overall, our findings extend the resistance spectrum of RdRP mice to retroviruses, utilizing FV infection as a model to investigate immune control of persistent viral infections.

The RdRP transgene protected mice from FV infection during the acute stages. We

FIG 7 Legend (Continued)
pre- and postinfection. Mice were sacrificed at 7 dpi for evaluation of FV infection. For all experiments shown, $n = 4$ for mock (uninfected WT mice, included to show baseline spleen size), $n = 8$ for WT with MAR1-5A or IgG, and $n = 7$ for RdRP with MAR1-5A or IgG. (B) qRT-PCR from liver sections for the mRNA of the representative ISG Oasl2. (C) Spleen weights of mice described in panel A. (D) Plasma viral load of mice described in panel A. Data were $\log_{10}$ transformed prior to analysis. (E, G) Spleen cell analyses. Shown are total FV-positive (FV^+) splenocytes (E) and FV^+ T cells, B cells, DCs, and erythroblasts (G) in the spleens of infected mice as determined by flow cytometry. (F, H) Bone marrow cell analyses. Shown are percent FV-positive total cells (F) and percent FV-positive T cells, B cells, DCs, and erythroblasts (H) in the bone marrows of infected mice as determined by flow cytometry. A one-way ANOVA followed by a Tukey's test to determine significance was used to analyze spleen weight and Oasl2 expression. All other data were analyzed using a two-way ANOVA followed by a Tukey's test to determine significance. *, $P < 0.05$; **, $P < 0.01$; ***, $P < 0.001$; ****, $P < 0.0001$.

further observed that lowering the FV inoculum dose revealed an antiviral effect of the RdRP in the bone marrow (Fig. 5D and F), suggesting that RdRP likely inhibited early FV infection through yet-to-be-identified saturable factors. Studies using IFNAR knockout (KO) mice demonstrate that type I IFN signaling is critical for inhibiting FV infection *in vivo* (25). IFNAR signaling triggers many antiviral genes. Using the anti-IFNAR antibody MAR1-5A, we demonstrate that neutralizing the ISG signature in RdRP mice blocks protection from FV infection and simultaneously downregulates Oasl2 expression as well (Fig. 7). These data indicate that ongoing type I IFN signaling is required to maintain ISG augmentation and FV protection. Previous studies in RdRP mice have shown that hundreds of ISGs in multiple antiviral pathways are elevated in these mice (5). It is likely that many ISGs act at a number of different stages of the FV life cycle to limit viral infection and spread.

The most well-characterized and understood host protein that affects FV infection is murine apolipoprotein B mRNA-editing enzyme, catalytic polypeptide-like (APOBEC) 3 (mA3) (31, 32). Compared to WT mice, mA3 KO mice exhibited higher FV infection levels (31, 45, 46). Moreover, the antiretroviral effects of exogenously administered IFN-α were abrogated in mA3 KO mice (47). Interestingly, it was also shown that mA3 inhibited FV infection independent of IFNAR (48). The mA3 gene in FVB mice is the full-length, biologically attenuated form compared to that found in C57BL strains of mice. This raised the question of what other restriction factors, such as Tetherin/BST-2, may be involved in inhibiting FV infection in RdRP mice. In Fig. 2 and 4, we showed that, in fact, a number of ISGs are elevated in both the spleen and bone marrow, including BST-2. This again confirms that a broad range of ISGs upregulated in different tissues of RdRP mice are mediating protection from FV infection. Studies into less well-described genes upregulated in RdRP mice would be of interest in the future for identifying novel antiviral factors.

We also observed a protective effect of the RdRP genotype during the chronic stages of FV infection. In contrast to the acute stages, at later postinfection time points, adaptive immune responses play important roles. It is interesting that our data suggest that the presence of the RdRP may act to reduce the FV set point during chronic infection. Viral set point refers to the equilibrium between virus and host that is established during chronic infection with viruses such as HIV-1 (40, 49, 50). The host immune system is able to partially control, but not clear, the virus, maintaining replication at a fairly constant level. The set point is highly clinically relevant for HIV-1 pathogenesis, as it strongly determines HIV disease progression (40). Current models suggest that changes in this asymptomatic phase balance point between the human host and HIV-1 are driven largely by the adaptive immune system (51–55). Major histocompatibility complex (MHC) alleles that allow for better peptide presentation and a strong cytotoxic T cell response are the main drivers of a lower viral set point and delayed disease progression (51–55). Similarly, in Friend virus infection, protective MHC alleles that confer resistance have been reported (21, 56, 57). Interestingly, in this RdRP mouse model, which is characterized by a predominantly innate as opposed to adaptive immune system augmentation, we found that RdRP mice, but not their WT counterparts, had some recovery from viremia during chronic infection (Fig. 6D). The mechanism(s) remains unclear, and adaptive immune system variables may be operative too. One possibility is that RdRP-induced antiviral ISGs act continuously to restrain viral replication. They may also or alternatively inhibit acute FV infection, which then reduces FV-induced immunosuppression (30), resulting in a more potent adaptive immune response. It will be valuable to evaluate the induction of T cell and neutralizing antibody responses in RdRP mice infected with FV to evaluate the role of the adaptive response in viral control.

As to the possibility that the sustained antiviral ISG expression in RdRP mice may be sufficient for inhibiting chronic infection, our results suggest that FV infection decreased ISG expression in RdRP mice, but even these relatively reduced levels of antiviral ISG expression are likely to be protective. Our previous EMCV infections of *Rag1*$^{-/-}$ RdRP mice have shown that antiviral protection is independent of the

adaptive immune system (5). Thus, it is possible that experiments in such mice would show that RdRP mice can similarly control FV infection independently of adaptive immunity.

This work indicates that chronic activation of innate immune genes acts early to reduce viral burden and lessen disease symptoms, with lasting effects on chronic viral infection time points. A number of human pathogens, including the retroviruses HIV-1 and HTLV-1, establish lifelong infection. If a therapeutic could be created to temporarily boost the innate immune system in individuals at risk of contracting a retroviral infection, similar to the RdRP mice, viral control or viral resistance could potentially be established. Even if full immunity is not possible, predictive models indicate that a treatment that reduces and delays disease symptoms during chronic viral infection, as observed in RdRP mice, would be clinically beneficial (58). Work to determine what the immunostimulatory pathogen-associated molecular patterns (PAMPs) synthesized by the RdRP are is of interest for potential design of novel therapeutics. Development and use of new immunostimulatory molecules could form the basis for efficacious alternatives to agents such as polyinosinic-poly(C), which is presently being tested as a therapeutic for chronic hepatitis C infection (59). Work is in progress to understand how the constitutive MDA5 response and resulting major ISG elevations generated by low-level expression of the RdRP confer resistance without producing autoinflammatory outcomes.

MATERIALS AND METHODS

Mice. FVB mice were purchased from Jackson Laboratory. RdRP-FVB mice have been described previously (5). Mice were maintained as homozygous knock-ins on an FVB genetic background. Mice were handled in accordance with IACUC guidelines for the University of Colorado Denver, Anschutz Medical Center.

Infections. Mice of mixed gender were used between 12 and 20 weeks for infection. Within infection groups, as much as possible, mice were age matched and/or littermates. All infection groups used mixed-gender mice. Mice were anesthetized and inoculated via retro-orbital puncture with B-tropic virus (100 to 10,000 PFU) diluted in 300 μl Dulbecco modified Eagle medium (DMEM) media. Lactase dehydrogenase-elevating virus-free stocks of FV were prepared in BALB/c mice and titers were determined as described previously (48).

Antibody treatment. Mice were administered purified, low-endotoxin functional-grade anti-IFNAR antibody MAR1-5A or IgG control antibody (Leinco Technologies, Inc.) via intraperitoneal injection 6 days prior to, 2 days prior to, and 5 days post-FV infection. Mice were sacrificed at 7 dpi for evaluation of FV pathogenesis. An initial saturating dose of 2.5 mg/mouse antibody was administered with follow-up doses of 0.5 mg/mouse administered as described. Determination of dosing was based on manufacturer recommendations.

Flow cytometry. Analysis of infection and cellular populations in the spleen and bone marrow was conducted using a BD LSRII collecting 500,000 to 1,000,000 events per sample as previously described (35, 48). Briefly, samples were stained with mAB34 (monoclonal mouse anti-FV matrix from a hybridoma cell line) proceeded by the following antibodies: fluorescein isothiocyanate (FITC) anti-mouse Ter119 (eBioscience; catalog no. 11-5921-85), PerCP Cy5.5 anti-mouse CD19 (BioLegend; catalog no. 115534), Alexa Fluor700 anti-mouse CD3 (BD Bioscience; catalog no. 561388), PE-Cy7 anti-mouse CD11c (eBioscience; product no. 25-0114-82), and APC goat anti-mouse IgG2b (Columbia Bioscience; catalog no. D3-112-2b). For analysis of uninfected splenocytes, the above flow panel was used with APC anti-mouse NKp46 (BioLegend; catalog no. 137608) instead of FV-specific staining and Pacific Blue anti-mouse BST-2 (BioLegend; catalog no. 127108). For analysis of DC populations in uninfected mice, the following antibody panel was used: FITC anti-mouse CD19 (BioLegend; catalog no. 152404), FITC anti-mouse CD3 (BioLegend; catalog no. 100204), FITC anti-mouse NKp46 (BioLegend; catalog no. 137606), FITC anti-mouse Ly-6G (BioLegend; catalog no. 127606), Brilliant Violet 605 anti-mouse Ly-6C (BioLegend; catalog no. 128035), Brilliant Violet 711 anti-mouse CD8α (BioLegend; catalog no. 100759), PE anti-mouse Siglec H (BioLegend; catalog no. 129606), APC anti-mouse CD11c (BioLegend; catalog no. 117310), Brilliant Violet 421 anti-mouse CD11b (BioLegend; catalog no. 101235), PerCP Cy5.5 anti-mouse CD80 (BioLegend; catalog no. 104722), PerCP Cy5.5 anti-mouse CD86 (BioLegend; catalog no. 105028), and fixable viability dye eFluor 780 (eBioscience; catalog no. 65-0865-14). Splenocytes were red blood cell depleted using red blood cell (RBC) lysis buffer (eBioscience) according to the manufacturer's instructions. Live/dead staining was done before surface staining according to the manufacturer's instructions (eFluor 780). Data were analyzed using FlowJo software, and gates were set based on uninfected or isotype stained samples. For DC/monocyte panel, gating was set based on fluorescence minus one controls. Cells were gated to exclude doublets, dead cells, and exclude lineage-positive cells (CD19 positive [CD19$^+$], CD3$^+$, NKp46$^+$, and Ly-6G$^+$). For individual cell populations, pDCs were gated as Siglec H$^+$ cells. Siglec H-negative (Siglec H$^-$) cells were gated for Ly-6C$^+$ (monocytes) or Ly-6C$^-$. Ly-6C$^-$ cells were gated as CD8α^+, CD11c$^+$ (cDC1s) and CD8α^-, CD11c$^+$. CD8α^- and CD11c$^+$ were gated as CD11c^{hi}, CD11b^{lo} (cDC2s), and CD11c^{lo} CD11b^{hi} (monocyte-derived DCs [moDCs]). For experiments where total cell count is shown, percentages were normalized to spleen weight using the conversion of 100 mg spleen = 10^8 splenocytes (60).

Plasma viral load. Plasma viral load (PVL) was determined as previously described (35, 48). Briefly, RNA was isolated from 50 μl plasma using an RNeasy plus minikit (Qiagen) according to the kit protocol and eluted in 50 μl RNase-free water. RNA was amplified and quantified using a Luna universal probe 1-step RT-qPCR kit (NEB) with the following 8-pmol primers: forward, 5′-GGACAGAAACTACCGCCCTG-3′, and reverse, 5′-ACAACCTCAGACAACGAAGTAAGA-3′, and the 4-pmol probe 6-carboxyfluorescein (FAM)-TCGCCACCCAGCAGTTTCAGCAGC-6-carboxytetramethylrhodamine (TAMRA). Copy number was determined compared to a plasmid standard. For all experiments, at least one uninfected control mouse serum was tested in parallel, and all uninfected samples tested resulted in undetectable FV RNA, so the data were excluded from comparisons.

qPCR measurements of mRNA levels. Ifit1, Isg15, and Oasl2 mRNAs were chosen as representative major mouse ISGs that have reliable primer sets for qPCR measurements, not because they are known to be particularly contributory to the aggregate antiviral effect among the many ISGs (over 100) that are constitutively elevated in the RdRP mouse. RNA was isolated from spleen using Trizol (Ambion) by use of the extraction method listed in the manufacturer's instructions. For bone marrow RNA, extractions were done using an RNeasy kit (Qiagen) according to the manufacturer's instructions. cDNA was synthesized using Maxima H Minus first strand cDNA synthesis kit (Thermo Scientific) according to the kit instructions. qPCR to quantify cellular transcripts was done using 2× qPCR master mix green (Apex) and the primers 5′-CATGGCCTTCCGTGTTCCTA-3′ and 5′-CTATGTTTCCCGCGGCACGTCAGATCCA-3′ for glyceraldehyde-3-phosphate dehydrogenase (GAPDH), 5′-TTTGTTGTTGTTGTTGTTCGTT-3′ and 5′-GCAG GAATCAGTTGTGATCT-3′ for Ifit1, 5′-TGGTACAGAACTGCAGCGAG-3′ and 5′-CAGCCAGAACTGGTCTTCG T-3′ for Isg15, and 5′-CAAACAAACAAACAAACCCTCTC-3′ and 5′-TCAAGGTGTCACTCTGCAT-3′ for Oasl2. For measurements of RdRP transgene mRNA levels, the primers were 5′-AGTGCTGTCACGCTATGACC-3′ and 5′-GAAGGTCGGTTCGTCTAAGT-3′. For proinflammatory cytokines, primers were 5′-CCGGAGAGGAG ACTTCACAG-3′ and 5′-TCCACGATTTCCCAGAGAAC-3′ for IL-6 and 5′-ACGGCATGGATCTCAAAGAC-3′ and 5′-GTGGGTGAGGAGCACGTAGT-3′ for TNF-α. Relative amounts of transcripts were quantified using the $\Delta\Delta C_T$ (threshold cycle) method with GAPDH as an internal control.

Statistical analysis. All statistical analyses were conducted using GraphPad Prism 8.2. As indicated, data were analyzed using a two-tailed, unpaired Student's *t* test (two-group comparisons), a one-way analysis of variance (ANOVA) followed by a Tukey's multiple-comparison test to determine adjusted *P* values, or a two-way ANOVA followed by a Tukey's test for multiple comparisons to determine adjusted *P* values. All plasma viral load data were log transformed prior to statistical analysis since standards for comparison were made in 10-fold dilutions. Data were tested for normalcy using a Shapiro-Wilk normalcy test, and data found to be non-Gaussian were analyzed with a Kruskal-Wallis test followed by Dunn's multiple-comparison test to determine significance thresholds (multiple group comparisons). On occasion, Grubb's test was used to detect and eliminate data outliers. For correlation analysis, all plasma viral load data were log transformed, and correlation analysis and a Pearson's test were used to determine the correlation between plasma viral load and spleen weight.

ACKNOWLEDGMENTS

The work was supported by NIH Avant-Garde grant DP1 DA043915 (E.M.P.), a Tietze Foundation grant (E.M.P.), and NIH R01 AI116603 (M.L.S.). The University of Colorado Anschutz Medical Campus flow cytometry core is supported by a National Cancer Institute grant (P30CA046934).

We thank Laura Bankers for transcriptome sequencing (RNA-seq) determinations of RdRP mRNA levels.

REFERENCES

1. Crow YJ, Manel N. 2015. Aicardi-Goutières syndrome and the type I interferonopathies. Nat Rev Immunol 15:429–440. https://doi.org/10.1038/nri3850.
2. Schneider WM, Chevillotte MD, Rice CM. 2014. Interferon-stimulated genes: a complex web of host defenses. Annu Rev Immunol 32:513–545. https://doi.org/10.1146/annurev-immunol-032713-120231.
3. Wu J, Chen ZJ. 2014. Innate immune sensing and signaling of cytosolic nucleic acids. Annu Rev Immunol 32:461–488. https://doi.org/10.1146/annurev-immunol-032713-120156.
4. Lee-Kirsch MA. 2017. The type I interferonopathies. Annu Rev Med 68:297–315. https://doi.org/10.1146/annurev-med-050715-104506.
5. Painter MM, Morrison JH, Zoecklein LJ, Rinkoski TA, Watzlawik JO, Papke LM, Warrington AE, Bieber AJ, Matchett WE, Turkowski KL, Poeschla EM, Rodriguez M. 2015. Antiviral protection via RdRP-mediated stable activation of innate immunity. PLoS Pathog 11:e1005311. https://doi.org/10.1371/journal.ppat.1005311.
6. Kerkvliet J, Zoecklein L, Papke L, Denic A, Bieber AJ, Pease LR, David CS, Rodriguez M. 2009. Transgenic expression of the 3D polymerase inhibits Theiler's virus infection and demyelination. J Virol 83:12279–12289. https://doi.org/10.1128/JVI.00664-09.
7. Kerkvliet J, Papke L, Rodriguez M. 2011. Antiviral effects of a transgenic RNA-dependent RNA polymerase. J Virol 85:621–625. https://doi.org/10.1128/JVI.01626-10.
8. Bienz K, Egger D, Pfister T, Troxler M. 1992. Structural and functional characterization of the poliovirus replication complex. J Virol 66:2740–2747. https://doi.org/10.1128/JVI.66.5.2740-2747.1992.
9. Romero-Brey I, Bartenschlager R. 2014. Membranous replication factories induced by plus-strand RNA viruses. Viruses 6:2826–2857. https://doi.org/10.3390/v6072826.
10. Varmus H. 1988. Retroviruses. Science 240:1427–1435. https://doi.org/10.1126/science.3287617.
11. Gibbert K, Francois S, Sigmund AM, Harper MS, Barrett BS, Kirchning CJ, Lu M, Santiago ML, Dittmer U. 2014. Friend retrovirus drives cytotoxic effectors through Toll-like receptor 3. Retrovirology 11:126. https://doi.org/10.1186/s12977-014-0126-4.
12. Kane M, Case LK, Wang C, Yurkovetskiy L, Dikiy S, Golovkina TV. 2011. Innate immune sensing of retroviral infection via Toll-like receptor 7 occurs upon viral entry. Immunity 35:135–145. https://doi.org/10.1016/j.immuni.2011.05.011.
13. Browne EP. 2011. Toll-like receptor 7 controls the anti-retroviral germinal center response. PLoS Pathog 7:e1002293. https://doi.org/10.1371/journal.ppat.1002293.

14. Gao D, Wu J, Wu YT, Du F, Aroh C, Yan N, Sun L, Chen ZJ. 2013. Cyclic GMP-AMP synthase is an innate immune sensor of HIV and other retroviruses. Science 341:903–906. https://doi.org/10.1126/science.1240933.
15. Monroe KM, Yang Z, Johnson JR, Geng X, Doitsh G, Krogan NJ, Greene WC. 2014. IFI16 DNA sensor is required for death of lymphoid CD4 T cells abortively infected with HIV. Science 343:428–432. https://doi.org/10.1126/science.1243640.
16. Stavrou S, Blouch K, Kotla S, Bass A, Ross SR. 2015. Nucleic acid recognition orchestrates the anti-viral response to retroviruses. Cell Host Microbe 17:478–488. https://doi.org/10.1016/j.chom.2015.02.021.
17. Kumar S, Morrison J, Dingli D, Poeschla E. 2018. HIV-1 induction of interferon-stimulated genes depends strongly on intracellular levels of TREX1 and sensing of incomplete reverse transcription products. J Virol 92:e00001-18. https://doi.org/10.1128/JVI.00001-18.
18. Miyazawa M, Tsuji-Kawahara S, Kanari Y. 2008. Host genetic factors that control immune responses to retrovirus infections. Vaccine 26:2981–2996. https://doi.org/10.1016/j.vaccine.2008.01.004.
19. Maetzig T, Galla M, Baum C, Schambach A. 2011. Gammaretroviral vectors: biology, technology and application. Viruses 3:677–713. https://doi.org/10.3390/v3060677.
20. Panfil AR, Al-Saleem JJ, Green PL. 2013. Animal models utilized in HTLV-1 research. Virology (Auckl) 4:49–59. https://doi.org/10.4137/VRT.S12140.
21. Hasenkrug KJ, Chesebro B. 1997. Immunity to retroviral infection: the Friend virus model. Proc Natl Acad Sci U S A 94:7811–7816. https://doi.org/10.1073/pnas.94.15.7811.
22. Persons DA, Paulson RF, Loyd MR, Herley MT, Bodner SM, Bernstein A, Correll PH, Ney PA. 1999. Fv2 encodes a truncated form of the Stk receptor tyrosine kinase. Nat Genet 23:159–165. https://doi.org/10.1038/13787.
23. Dittmer U, Sutter K, Kassiotis G, Zelinskyy G, Banki Z, Stoiber H, Santiago ML, Hasenkrug KJ. 2019. Friend retrovirus studies reveal complex interactions between intrinsic, innate and adaptive immunity. FEMS Microbiol Rev 43:435–456. https://doi.org/10.1093/femsre/fuz012.
24. Taketo M, Schroeder AC, Mobraaten LE, Gunning KB, Hanten G, Fox RR, Roderick TH, Stewart CL, Lilly F, Hansen CT. 1991. FVB/N: an inbred mouse strain preferable for transgenic analyses. Proc Natl Acad Sci U S A 88:2065–2069. https://doi.org/10.1073/pnas.88.6.2065.
25. Gerlach N, Schimmer S, Weiss S, Kalinke U, Dittmer U. 2006. Effects of type I interferons on Friend retrovirus infection. J Virol 80:3438–3444. https://doi.org/10.1128/JVI.80.7.3438-3444.2006.
26. Ammann CG, Messer RJ, Peterson KE, Hasenkrug KJ. 2009. Lactate dehydrogenase-elevating virus induces systemic lymphocyte activation via TLR7-dependent IFNalpha responses by plasmacytoid dendritic cells. PLoS One 4:e6105. https://doi.org/10.1371/journal.pone.0006105.
27. Ruscetti SK. 1999. Deregulation of erythropoiesis by the Friend spleen focus-forming virus. Int J Biochem Cell Biol 31:1089–1109. https://doi.org/10.1016/s1357-2725(99)00074-6.
28. Banerjee P, Crawford L, Samuelson E, Feuer G. 2010. Hematopoietic stem cells and retroviral infection. Retrovirology 7:8. https://doi.org/10.1186/1742-4690-7-8.
29. Ruscetti SK. 1995. Erythroleukaemia induction by the Friend spleen focus-forming virus. Baillieres Clin Haematol 8:225–247. https://doi.org/10.1016/s0950-3536(05)80239-2.
30. Dittmer U, He H, Messer RJ, Schimmer S, Olbrich AR, Ohlen C, Greenberg PD, Stromnes IM, Iwashiro M, Sakaguchi S, Evans LH, Peterson KE, Yang G, Hasenkrug KJ. 2004. Functional impairment of CD8+ T cells by regulatory T cells during persistent retroviral infection. Immunity 20:293–303. https://doi.org/10.1016/s1074-7613(04)00054-8.
31. Santiago ML, Montano M, Benitez R, Messer RJ, Yonemoto W, Chesebro B, Hasenkrug KJ, Greene WC. 2008. Apobec3 encodes Rfv3, a gene influencing neutralizing antibody control of retrovirus infection. Science 321:1343–1346. https://doi.org/10.1126/science.1161121.
32. Santiago ML, Smith DS, Barrett BS, Montano M, Benitez RL, Pelanda R, Hasenkrug KJ, Greene WC. 2011. Persistent Friend virus replication and disease in Apobec3-deficient mice expressing functional B-cell-activating factor receptor. J Virol 85:189–199. https://doi.org/10.1128/JVI.01838-10.
33. Chesebro B, Wehrly K. 1979. Identification of a non-H-2 gene (Rfv-3) influencing recovery from viremia and leukemia induced by Friend virus complex. Proc Natl Acad Sci U S A 76:425–429. https://doi.org/10.1073/pnas.76.1.425.
34. Barrett BS, Smith DS, Li SX, Guo K, Hasenkrug KJ, Santiago ML. 2012. A single nucleotide polymorphism in tetherin promotes retrovirus restriction in vivo. PLoS Pathog 8:e1002596. https://doi.org/10.1371/journal.ppat.1002596.
35. Li SX, Barrett BS, Heilman KJ, Messer RJ, Liberatore RA, Bieniasz PD, Kassiotis G, Hasenkrug KJ, Santiago ML. 2014. Tetherin promotes the innate and adaptive cell-mediated immune response against retrovirus infection in vivo. J Immunol 193:306–316. https://doi.org/10.4049/jimmunol.1400490.
36. Neil SJ, Zang T, Bieniasz PD. 2008. Tetherin inhibits retrovirus release and is antagonized by HIV-1 Vpu. Nature 451:425–430. https://doi.org/10.1038/nature06553.
37. Van Damme N, Goff D, Katsura C, Jorgenson RL, Mitchell R, Johnson MC, Stephens EB, Guatelli J. 2008. The interferon-induced protein BST-2 restricts HIV-1 release and is downregulated from the cell surface by the viral Vpu protein. Cell Host Microbe 3:245–252. https://doi.org/10.1016/j.chom.2008.03.001.
38. Geissmann F. 2007. The origin of dendritic cells. Nat Immunol 8:558–560. https://doi.org/10.1038/ni0607-558.
39. Geissmann F, Manz MG, Jung S, Sieweke MH, Merad M, Ley K. 2010. Development of monocytes, macrophages, and dendritic cells. Science 327:656–661. https://doi.org/10.1126/science.1178331.
40. Mellors JW, Rinaldo CR, Jr, Gupta P, White RM, Todd JA, Kingsley LA. 1996. Prognosis in HIV-1 infection predicted by the quantity of virus in plasma. Science 272:1167–1170. https://doi.org/10.1126/science.272.5265.1167.
41. Hwang SY, Hertzog PJ, Holland KA, Sumarsono SH, Tymms MJ, Hamilton JA, Whitty G, Bertoncello I, Kola I. 1995. A null mutation in the gene encoding a type I interferon receptor component eliminates antiproliferative and antiviral responses to interferons alpha and beta and alters macrophage responses. Proc Natl Acad Sci U S A 92:11284–11288. https://doi.org/10.1073/pnas.92.24.11284.
42. Sheehan KC, Lai KS, Dunn GP, Bruce AT, Diamond MS, Heutel JD, Dungo-Arthur C, Carrero JA, White JM, Hertzog PJ, Schreiber RD. 2006. Blocking monoclonal antibodies specific for mouse IFN-alpha/beta receptor subunit 1 (IFNAR-1) from mice immunized by in vivo hydrodynamic transfection. J Interferon Cytokine Res 26:804–819. https://doi.org/10.1089/jir.2006.26.804.
43. Rice GI, Del Toro Duany Y, Jenkinson EM, Forte GM, Anderson BH, Ariaudo G, Bader-Meunier B, Baildam EM, Battini R, Beresford MW, Casarano M, Chouchane M, Cimaz R, Collins AE, Cordeiro NJ, Dale RC, Davidson JE, De Waele L, Desguerre I, Faivre L, Fazzi E, Isidor B, Lagae L, Latchman AR, Lebon P, Li C, Livingston JH, Lourenço CM, Mancardi MM, Masurel-Paulet A, McInnes IB, Menezes MP, Mignot C, O'Sullivan J, Orcesi S, Picco PP, Riva E, Robinson RA, Rodriguez D, Salvatici E, Scott C, Szybowska M, Tolmie JL, Vanderver A, Vanhulle C, Vieira JP, Webb K, Whitney RN, Williams SG, Wolfe LA, Zuberi SM, Hur S, Crow YJ. 2014. Gain-of-function mutations in IFIH1 cause a spectrum of human disease phenotypes associated with upregulated type I interferon signaling. Nat Genet 46:503–509. https://doi.org/10.1038/ng.2933.
44. Funabiki M, Kato H, Miyachi Y, Toki H, Motegi H, Inoue M, Minowa O, Yoshida A, Deguchi K, Sato H, Ito S, Shiroishi T, Takeyasu K, Noda T, Fujita T. 2014. Autoimmune disorders associated with gain of function of the intracellular sensor MDA5. Immunity 40:199–212. https://doi.org/10.1016/j.immuni.2013.12.014.
45. Takeda E, Tsuji-Kawahara S, Sakamoto M, Langlois MA, Neuberger MS, Rada C, Miyazawa M. 2008. Mouse APOBEC3 restricts friend leukemia virus infection and pathogenesis in vivo. J Virol 82:10998–11008. https://doi.org/10.1128/JVI.01311-08.
46. Smith DS, Guo K, Barrett BS, Heilman KJ, Evans LH, Hasenkrug KJ, Greene WC, Santiago ML. 2011. Noninfectious retrovirus particles drive the APOBEC3/Rfv3 dependent neutralizing antibody response. PLoS Pathog 7:e1002284. https://doi.org/10.1371/journal.ppat.1002284.
47. Harper MS, Barrett BS, Smith DS, Li SX, Gibbert K, Dittmer U, Hasenkrug KJ, Santiago ML. 2013. IFN-alpha treatment inhibits acute Friend retrovirus replication primarily through the antiviral effector molecule Apobec3. J Immunol 190:1583–1590. https://doi.org/10.4049/jimmunol.1202920.
48. Barrett BS, Harper MS, Jones ST, Guo K, Heilman KJ, Kedl RM, Hasenkrug KJ, Santiago ML. 2017. Type I interferon signaling is required for the APOBEC3/Rfv3-dependent neutralizing antibody response but not innate retrovirus restriction. Retrovirology 14:25. https://doi.org/10.1186/s12977-017-0349-2.
49. Mellors JW, Munoz A, Giorgi JV, Margolick JB, Tassoni CJ, Gupta P, Kingsley LA, Todd JA, Saah AJ, Detels R, Phair JP, Rinaldo CR, Jr. 1997. Plasma viral load and CD4+ lymphocytes as prognostic markers of HIV-1 infection. Ann Intern Med 126:946–954. https://doi.org/10.7326/0003-4819-126-12-199706150-00003.
50. McMichael AJ, Borrow P, Tomaras GD, Goonetilleke N, Haynes BF. 2010. The

immune response during acute HIV-1 infection: clues for vaccine development. Nat Rev Immunol 10:11–23. https://doi.org/10.1038/nri2674.
51. Borrow P, Lewicki H, Hahn BH, Shaw GM, Oldstone MB. 1994. Virus-specific CD8+ cytotoxic T-lymphocyte activity associated with control of viremia in primary human immunodeficiency virus type 1 infection. J Virol 68:6103–6110. https://doi.org/10.1128/JVI.68.9.6103-6110.1994.
52. Streeck H, Jolin JS, Qi Y, Yassine-Diab B, Johnson RC, Kwon DS, Addo MM, Brumme C, Routy JP, Little S, Jessen HK, Kelleher AD, Hecht FM, Sekaly RP, Rosenberg ES, Walker BD, Carrington M, Altfeld M. 2009. Human immunodeficiency virus type 1-specific CD8+ T-cell responses during primary infection are major determinants of the viral set point and loss of CD4+ T cells. J Virol 83:7641–7648. https://doi.org/10.1128/JVI.00182-09.
53. Deeks SG, Kitchen CM, Liu L, Guo H, Gascon R, Narvaez AB, Hunt P, Martin JN, Kahn JO, Levy J, McGrath MS, Hecht FM. 2004. Immune activation set point during early HIV infection predicts subsequent CD4+ T-cell changes independent of viral load. Blood 104:942–947. https://doi.org/10.1182/blood-2003-09-3333.
54. Koup RA, Safrit JT, Cao Y, Andrews CA, McLeod G, Borkowsky W, Farthing C, Ho DD. 1994. Temporal association of cellular immune responses with the initial control of viremia in primary human immunodeficiency virus type 1 syndrome. J Virol 68:4650–4655. https://doi.org/10.1128/JVI.68.7.4650-4655.1994.
55. O'Brien SJ, Nelson GW. 2004. Human genes that limit AIDS. Nat Genet 36:565–574. https://doi.org/10.1038/ng1369.
56. Chesebro B, Wehrly K, Stimpfling J. 1974. Host genetic control of recovery from Friend leukemia virus-induced splenomegaly: mapping of a gene within the major histocompatability complex. J Exp Med 140:1457–1467. https://doi.org/10.1084/jem.140.6.1457.
57. Chesebro B, Wehrly K. 1978. Rfv-1 and Rfv-2, two H-2-associated genes that influence recovery from Friend leukemia virus-induced splenomegaly. J Immunol 120:1081–1085.
58. Gupta SB, Jacobson LP, Margolick JB, Rinaldo CR, Phair JP, Jamieson BD, Mehrotra DV, Robertson MN, Straus WL. 2007. Estimating the benefit of an HIV-1 vaccine that reduces viral load set point. J Infect Dis 195:546–550. https://doi.org/10.1086/510909.
59. Gane EJ, Lim YS, Gordon SC, Visvanathan K, Sicard E, Fedorak RN, Roberts S, Massetto B, Ye Z, Pflanz S, Garrison KL, Gaggar A, Mani Subramanian G, McHutchison JG, Kottilil S, Freilich B, Coffin CS, Cheng W, Kim YJ. 2015. The oral toll-like receptor-7 agonist GS-9620 in patients with chronic hepatitis B virus infection. J Hepatol 63:320–328. https://doi.org/10.1016/j.jhep.2015.02.037.
60. Barrett BS, Guo K, Harper MS, Li SX, Heilman KJ, Davidson NO, Santiago ML. 2014. Reassessment of murine APOBEC1 as a retrovirus restriction factor in vivo. Virology 468–470:601–608. https://doi.org/10.1016/j.virol.2014.09.006.